Electrostatic Analysis of Charge Interactions in Proteins

G. P. TSIRONIS,[1,2] **A. CIUDAD,**[1] **J. M. SANCHO**[1]

[1]*Department d' Estructura i Constituents de la Matéria, Facultat de Física, Universitat de Barcelona, Diagonal 647, E-08028 Barcelona, Spain*
[2]*Department of Physics, University of Crete and Institute of Electronic Structure and Laser, FORTH, P. O. Box 2208, Heraklion 71003, Crete, Greece*

Received 26 October 2008; accepted 13 January 2009
Published online 19 May 2009 in Wiley InterScience (www.interscience.wiley.com).
DOI 10.1002/qua.22123

ABSTRACT: We model proteins as continuous electrostatic media immersed in water to investigate charge mediated processes in their interior. We use a Green's function formalism and find analytical expressions for the electrostatic energy in the vicinity of the protein surfaces. We find that due to image charges generated by the protein dielectric medium embedded in water, the effective electrostatic interaction between the two charges in the interior of the protein has an energy larger than the thermal energy. We focus specifically on kinesin to asses the strength of the electrostatic interaction between ATP and ADP molecules. It is known experimentally that ADP expulsion is correlated to ATP kinesin binding while both processes are essential for the kinesin walk. We estimate that the Bjerrum length in the interior of the kinesin dimer protein is of the order of 4 nm and that the pure electrostatic ATP–ADP interaction is of the order of 3–5 k_BT. © 2009 Wiley Periodicals, Inc. Int J Quantum Chem 110: 233–241, 2010

Key words: protein electrostatics; charge transfer; kinesin walk; ATP–ADP interaction; Bjerrum length

1. Introduction

A large number of biological processes involve charge transfer from the exterior of a macromolecule to its interior. Because of the complex dielectric and shielding properties of both the macromolecules as well as their environment it is many times hard to asses the role electrostatic energy plays in these processes. For instance, one case of interest involves charged ATP entry in motor proteins such as kinesin that is accompanied by the expulsion of charged ADP found in distant locations within the protein [1, 2]. Other cases involve the so-called electrostatic switch that induces a phosph-dependent regulation or the entry of charges in

Correspondence to: G. P. Tsironis; e-mail: gts@physics.uco.gr
Contract grant sponsor: Ministerio de Educación y Ciencia (Spain).
Contract grant numbers: BES-2004-3208, 2006PIV10007.

the cell membrane [3, 4]. Macromolecules are complex, discrete networks that involve distributions of charges, dipoles, etc. To investigate electrostatic phenomena in such systems we assume that they comprise a continuous medium with a relative dielectric constant that has a small value, typically of the order $\epsilon \simeq 4$, whereas the surrounding medium has a large dielectric constant similar to that of water, viz. $\epsilon_{H_2O} \simeq 80$. What we are interested in analyzing is the effect the interfaces between the low and high dielectric media play in the energetics of charged molecules.

When a charge is placed in front of a dielectric embedded in a high permittivity medium the induced image charges repel the charge and lead to a small field in the interior of the dielectric. When, on the other hand, this charge is placed just in the interior of the dielectric, the force-field changes drastically and the new force exerted is substantially larger. This is the process that is followed, for instance, during the ATP hydrolysis circle in a motor protein; whereas initially the ATP charge is exterior to protein, on entry and hydrolysis a local conformational change takes place that captures the charge in the protein interior that essentially excludes all water molecules. To estimate the change in the force, we will model the protein as an infinite dielectric with a given thickness d representing the longitudinal dimension of the dimeric protein. Although approximating a complex protein through a slab geometry presents a gross simplification of the problem, it nevertheless captures the essential effects the presence of interfaces have on the charge energetics within the protein [5, 6].

In the remaining of the article, we will describe the method of calculation in the following section and apply it to the interface of two dielectrics first and to a slab geometry subsequently. We will provide analytical expressions for the Green's functions and though these we will evaluate the scale of the Bjerrum length in the interior of the model protein. In the final section, we will focus more explicitly on kinesin, as one of the best known molecular motors and present quantitative estimates for the ATP–ADP interaction inside this protein.

2. Green's Function Method

We will evaluate the Greens function of the Poisson equation to calculate the force field generated by charges in the vicinity of the protein–water interface. We briefly outline the procedure [7] later. The Poisson equation is written as

$$\nabla^2\phi(\mathbf{r}) = -\frac{\rho(\mathbf{r})}{\epsilon} \tag{1}$$

where $\rho(\mathbf{r})$ is the charge density, $\epsilon = \epsilon_0\epsilon_r$, where ϵ_0 the vacuum dielectric permittivity whereas ϵ_r is the relative permittivity of the specific dielectric medium. The Green's function equation corresponding to Eq. (1) is

$$\nabla^2 G(\mathbf{r}, \mathbf{r}') = -\frac{1}{\epsilon}\delta(\mathbf{r} - \mathbf{r}') \tag{2}$$

Expanding the δ-function in the Fourier domain as

$$\delta(\mathbf{r} - \mathbf{r}') = \int \frac{\mathbf{dk}}{(\mathbf{2}\pi)^3} \mathbf{e}^{\mathbf{ik}\cdot(\mathbf{r}-\mathbf{r}')} \tag{3}$$

it is easy to see that the Green's function of Eq. (2) is

$$G(\mathbf{r}, \mathbf{r}') = \frac{1}{\epsilon}\int \frac{\mathbf{dk}}{(\mathbf{2}\pi)^3} \frac{\mathbf{e}^{\mathbf{ik}\cdot(\mathbf{r}-\mathbf{r}')}}{\mathbf{k^2}} = \frac{\mathbf{1}}{\mathbf{4}\pi\epsilon|\mathbf{r} - \mathbf{r}'|} \tag{4}$$

For a problem in which there are changes in only one (e.g., z) axis while the configuration is invariant in the other two, one may write the Green's function of Eq. (4) as

$$G(\mathbf{r}, \mathbf{r}') = \int \frac{\mathbf{dk}_\perp}{(\mathbf{2}\pi)^2} \mathbf{e}^{\mathbf{ik}_\perp\cdot(\mathbf{r}-\mathbf{r}')_\perp} \mathbf{g}(\mathbf{z}, \mathbf{z}'; \mathbf{k}_\perp) \tag{5}$$

with $\mathbf{k} = \mathbf{k}_\perp + \hat{z}k_z$ and where, upon substitution in Eq. (2) and use of Eq. (4) we obtain the following equation for the reduced Green's function $g(z, z'; k)$:

$$\left[k_\perp^2 - \frac{\partial^2}{\partial z^2}\right] g(z, z'; k) = \frac{1}{\epsilon}\delta(z - z') \tag{6}$$

When the reduced Green's function is evaluated through the solution of Eq. (6), the complete Green's function is found by direct substitution of the former in Eq. (5). It suffices thus to solve Eq. (6) and find the reduced Green's function to calculate the complete Green's function; performing the angular integration in Eq. (5) and using cylindrical coordinates, we find

$$G(\rho, z) = \frac{1}{2\pi}\int_0^\infty J_0(k\rho) g(z, z', k) k dk \tag{7}$$

where $J_0(z)$ is the Bessel function of zero order. We note that on the axis of the charge that is

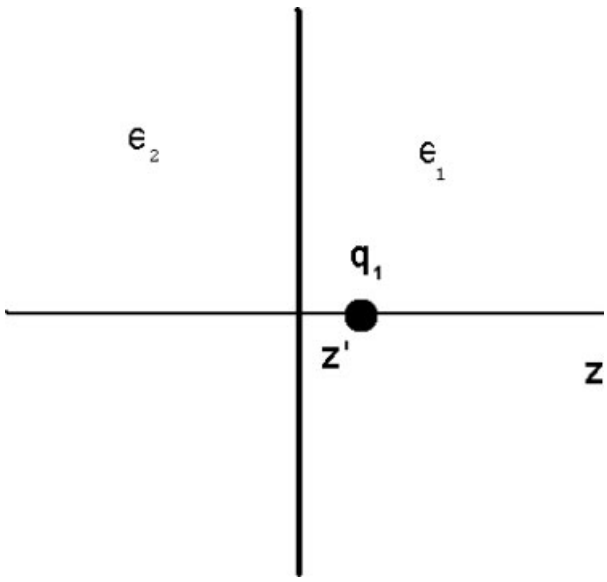

FIGURE 1. Two seminfinite dielectric media in which the first with relative dielectric permittivity ϵ_1 represents water whereas the second with ϵ_2 is a semi-infinite protein. The charge q_1 is located at a distance d from the water–protein interface.

perpendicular to the interface, i.e., for $\rho = 0$, the integral expression simplifies to

$$G(z) = \frac{1}{2\pi}\int_0^\infty g(z,z',k)kdk \tag{8}$$

3. Charge in Front of a Dielectric Interface

Let us first consider the simpler case of a charge placed in front of an infinite interface at $z = 0$ that separates two dielectric media (Fig. 1). The dielectric at $z > 0$ has relative permittivity ϵ_1 whereas the one at $z < 0$ has relative permittivity ϵ_2. We consider that the medium 2 is a protein with typical permittivity $\epsilon_2 \simeq 4$ whereas medium 1 is water with $\epsilon_1 \simeq 80$. We place a charge $q \equiv q_1$ in the water at distance d from the protein interface. We would like to calculate potentials and fields induced by the charge q in both media.

To find the Green's function in this simple case, we need first to solve Eq. (6) for the reduced Greens function in the direction z where the electric permittivity has a discontinuity across the interface. The boundary conditions on it are $E_\perp^{(1)} = E_\perp^{(2)}$ and $D_z^{(1)} = D_z^{(2)}$, or $\epsilon_1 E_z^{(1)} = \epsilon_2 E_z^{(2)}$. The calculation of $g(z,z';k)$ is simple in this case; we assume that the unit charge is placed at the point $z' > 0$, i.e., located in the medium with dielectric constant ϵ_1. The reduced Green's function takes the form

$$\begin{aligned} g(z,z';k) &= Ae^{-kz}, \quad z > z' \\ g(z,z';k) &= Be^{-kz} + Ce^{kz}, \quad z' \le z < 0 \\ g(z,z';k) &= De^{kz}, \quad 0 \ge z \end{aligned} \tag{9}$$

where $k \equiv k_\perp$. The Green's function $g(z,z';k)$ is continuous on the charge at z' whereas it has a derivative jump equal to $g'(z',z';k) = -1/\epsilon_1$. Using these facts and the boundary conditions at the interface leads easily to the following expression for the reduced Green's function:

$$\begin{aligned} g(z,z';k) &= \frac{1}{2k\epsilon_1}\left[e^{-k|z-z'|} + \frac{\epsilon_1-\epsilon_2}{\epsilon_1+\epsilon_2}e^{-k(z+z')}\right], \quad z \ge 0 \\ g(z,z';k) &= \frac{1}{2k\epsilon_1}\frac{2\epsilon_1}{\epsilon_1+\epsilon_2}e^{-k(z-z')}, \quad z \le 0 \end{aligned} \tag{10}$$

Use of Eq. (8) leads directly in the standard expressions for the potentials for the unit charge in front of dielectric interface [8]:

$$G(z,z') = \frac{1}{4\pi\epsilon_1}\left[\frac{1}{|z-z'|} + \frac{\epsilon_1-\epsilon_2}{\epsilon_1+\epsilon_2}\frac{1}{z+z'}\right], \quad z \ge 0 \tag{11}$$

$$G(z,z') = \frac{1}{4\pi}\frac{2}{\epsilon_1+\epsilon_2}\frac{1}{-k(z'-z)}, \quad z \le 0 \tag{12}$$

We note in passing that the two expressions for the reduced Green's functions of Eq. (10) for $z' > 0$ may be combined to the following expression:

$$g(z,z';k) = \frac{1}{2k\epsilon_1}\left[e^{-k|z-z'|} + \frac{\epsilon_1-\epsilon_2}{\epsilon_1+\epsilon_2}e^{-k(|z|+|z'|)}\right] \tag{13}$$

The expression for the reduced Green's function for the charge in the interior, i.e., for $z' < 0$ is obtained simply by multiplying the expression in Eq. (8) by ϵ_1/ϵ_2 and replace the z-coordinates by their negatives. The interaction energy of the charges as a function of the distances in the interior of the model protein is shown in Figure 2.

This exercise with a single dielectric interface shows that the Green's function method may be used straightforwardly for the calculation of potentials, fields as well as forces related to dielectric interfaces. Before we apply the method to the case of the dielectric slab mimicking the two bounding dielectric surfaces of protein, let us first do some quantitative

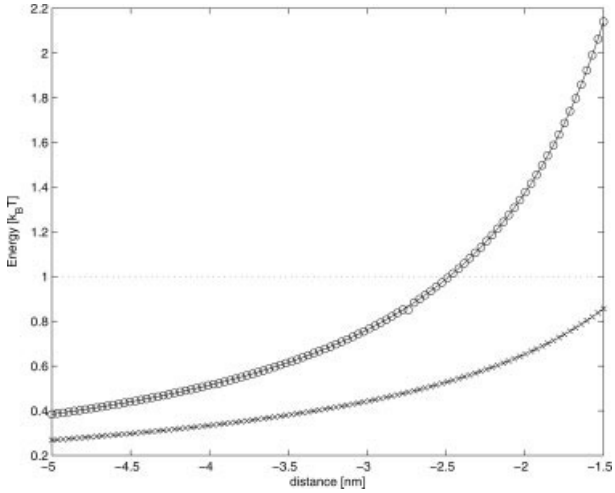

FIGURE 2. Energy in k_BT as a function of distance in *nm* for two unit charges near the interface that separates two media; medium 2 for $z < 0$ is a semi-infinite protein. Crosses were obtained numerically through numerical integration of Eq. (8) whereas the overlapping continuous curve is the exact result; both for the charge located at $z = 0.1$, i.e., in the exterior of the protein. Similarly circles and the overlapping continuous curve is for the charge in the interior of the protein at $z = -0.1$. The dotted horizontal line marks the room temperature energy k_BT.

estimates; specifically we will evaluate the role a single interface has to the electrostatic energy and force related to the charge-interface geometry.

To perform quantitative estimates, we assume that the charge is located on the z-axis at z' and has charge q_1 whereas the second charge is on the same axis at z and has charge q_2. Once the full Green's function is evaluated the electrostatic energy between the two charges is,

$$U = \frac{q_1 q_2}{4\pi\epsilon_0\epsilon_r}\frac{1}{|\mathbf{r}-\mathbf{r}'|} = \frac{q_1 q_2}{\epsilon_0}G(\rho, z) \tag{14}$$

Denoting $G \equiv G(\rho, z)$, and using units for charges in electron charges and distances in nm we may express the electrostatic energy as follows:

$$\begin{aligned} U &\simeq 2890 q_1 q_2 G \text{ [pN nm]} \\ &\simeq 18.0 q_1 q_2 G \text{ [eV]} \simeq 722.7 q_1 q_2 G \text{ [}k_BT\text{]} \end{aligned} \tag{15}$$

In case we need to calculate the force excerpted by charge q_1 on the charge q_2 we simply have to evaluate the derivative of the Green's function wrt to z; we denote the latter by G'. The force then is expressed as follows:

$$F = \frac{q_1 q_2}{\epsilon_0}G'(\rho, z) \tag{16}$$

leading to the following practical expression in pN:

$$F \simeq 230 q_1 q_2 G' \text{[pN]}$$

The above expressions for the energy and the force should be compared with the corresponding quantities for two charges embedded in a medium with relative dielectric permittivity ϵ_r. If we write the charges in units of electron charge and the distance in nm we have:

$$F \simeq \frac{230\,\text{pN}}{\epsilon_r}\frac{q_1 q_2}{r^2}$$

The electrostatic energy between two charges in an infinite medium is

$$E = \frac{1}{4\pi\epsilon_0\epsilon_r}\frac{q_1 q_2}{r},$$

and using electron charge and nm as units we have,

$$E \simeq \frac{230}{\epsilon_r}\frac{q_1 q_2}{r}\text{[pN nm]}$$

that may also be written as

$$E \simeq \frac{1.43}{\epsilon_r}\frac{q_1 q_2}{r}\text{[eV]} \simeq \frac{57.2}{\epsilon_r}\frac{q_1 q_2}{r}\ [k_BT].$$

4. Infinite Dielectric Slab

We model electrostatically a large protein as an infinite slab with length d and relative permittivity ϵ_2 located between $z = -d/2$ and $z = d/2$. The kinesin slab is embedded in a dielectric medium with much larger dielectric constant ϵ_2 (Fig. 3). We need to consider two cases with the charge interior and exterior to the slab.

We calculate the reduced Green's function in k-space using as boundary conditions the continuity of the electrostatic potential across each dielectric surface as well as the the continuity of the dielectric displacement across the interfaces. Additionally, we know that g is continuous at $z = z'$ in which the unit charge is located while it has a jump in its derivative with magnitude $-1/\epsilon_2$.

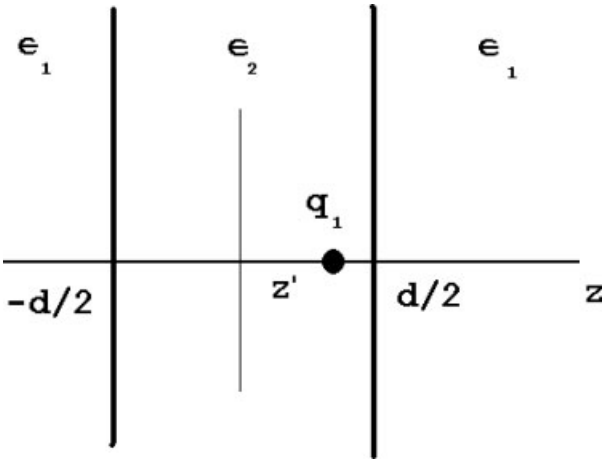

FIGURE 3. Infinite dielectric slab case in which the medium with dielectric constant ϵ_2 mimics a protein whereas ϵ_1 is the the dielectric constant of water. The distance d denotes the distance of the charge q_1 from the protein–water interface.

4.1. INTERIOR PROBLEM

We consider $-d/2 \le z' \le d/2$, The general expression for the reduced Greens function is:

$$g_I(z,z',k) = Ae^{-kz}, \quad z \ge d/2$$
$$g_{II,1}(z,z',k) = Be^{-kz} + Ce^{kz}, \quad z' \le z < d/2$$
$$g_{II,2}(z,z',k) = De^{-kz} + Ee^{kz}, \quad -d/2 \le z < z'$$
$$g_{III}(z,z',k) = Fe^{kz}, \quad z < -d/2 \tag{17}$$

Use of the boundary conditions anb the properties of g at $z = z'$ result to the following expressions for the coefficients:

$$E = \frac{1}{2k\epsilon_2\Delta}\left[(\epsilon_1+\epsilon_2)^2 e^{-kz'} - \left(\epsilon_1^2-\epsilon_2^2\right)e^{-k(d-z')}\right],$$
$$B = \frac{1}{2k\epsilon_2\Delta}\left[(\epsilon_1+\epsilon_2)^2 e^{kz'} - \left(\epsilon_1^2-\epsilon_2^2\right)e^{-k(d+z')}\right],$$
$$C = \frac{1}{2k\epsilon_2\Delta}\left[(\epsilon_1-\epsilon_2)^2 e^{-k(2d+z')} - \left(\epsilon_1^2-\epsilon_2^2\right)e^{-k(d-z')}\right],$$
$$D = \frac{1}{2k\epsilon_2\Delta}\left[(\epsilon_1-\epsilon_2)^2 e^{-k(2d-z')} - \left(\epsilon_1^2-\epsilon_2^2\right)e^{-k(d+z')}\right],$$
$$A = \frac{2\epsilon_2}{\epsilon_1+\epsilon_2}B, \quad F = \frac{2\epsilon_2}{\epsilon_1+\epsilon_2}E. \tag{18}$$

where

$$\Delta = (\epsilon_1+\epsilon_2)^2 - (\epsilon_1-\epsilon_2)^2 e^{-2kd}$$

Solution of this algebraic system and substitution to the Eq. (17) leads to the following exact expressions for the reduced Green's function for the interior problem:

$$g_I(z,z',k) = \frac{1}{k\Delta}\left[(\epsilon_1+\epsilon_2)e^{-k(z-z')} - (\epsilon_1-\epsilon_2)e^{-k(d+z+z')}\right], \quad z \ge \frac{d}{2}$$
$$g_{II}(z,z',k) = \frac{1}{2k\epsilon_2\Delta}\left[(\epsilon_1+\epsilon_2)^2 e^{-k|z-z'|} + (\epsilon_1-\epsilon_2)^2 e^{-(2d-|z-z'|)} - 2\left(\epsilon_1^2-\epsilon_2^2\right)e^{-kd}\cosh[k(z+z')]\right], \quad -\frac{d}{2} \le z \le \frac{d}{2}$$
$$g_{III}(z,z',k) = \frac{1}{k\Delta}\left[(\epsilon_1+\epsilon_2)e^{-k(z'-z)} - (\epsilon_1-\epsilon_2)e^{-k(d-z-z')}\right], \quad z < -\frac{d}{2} \tag{19}$$

These exact expressions may be used in conjunction with Eq. (17) to evaluate the interaction energies in the interior of the protein. We note that the expressions above involve direct potential terms as well as terms dependent on the effect of the interface.

4.2. EXTERIOR PROBLEM

Similarly, when we place the unit charge at point z' that is exterior to the slab and on the positive axis, viz. $z' \ge d/2$, we have

$$g_{I,1}(z,z',k) = Ae^{-kz}, \quad z \ge z'$$
$$g_{I,2}(z,z',k) = Be^{-kz} + Ce^{kz}, \quad \frac{d}{2} \le z < z'$$
$$g_{II}(z,z',k) = De^{-kz} + Ee^{kz}, \quad -\frac{d}{2} \le z < \frac{d}{2}$$
$$g_{III}(z,z',k) = Fe^{kz}, \quad z < -\frac{d}{2} \tag{20}$$

Application of the boundary conditions leads to,

$$C = \frac{1}{2k\epsilon_1}e^{-kz'},$$
$$F = \frac{2\epsilon_2 e^{-kz'}}{k\Delta},$$
$$B = \frac{\epsilon_1^2 - \epsilon_2^2}{k\epsilon_1\Delta}\sinh(kd)e^{-kz'},$$
$$A = \frac{\epsilon_1^2 - \epsilon_2^2}{k\epsilon_1\Delta}\sinh(kd)e^{-kz'} + \frac{1}{2k\epsilon_1}e^{kz'},$$
$$D = \frac{\epsilon_2 - \epsilon_1}{k\Delta}e^{-k(d+z')},$$
$$E = \frac{\epsilon_1 + \epsilon_2}{k\Delta}e^{-kz'} \tag{21}$$

Resolution of this algebraic system of equations and substitution to the Eq. (20) leads to the final expressions for the Green's function for the exterior problem;

$$g_I(z,z',k) = \frac{1}{2\epsilon_1 k}e^{-k|z'-z|} + \frac{1}{k\epsilon_1\Delta}\left(\epsilon_1^2 - \epsilon_2^2\right)\sinh(kd)e^{-k(z+z')}, \quad z \geq \frac{d}{2}$$
$$g_{II}(z,z',k) = \frac{1}{k\Delta}\left[(\epsilon_2 - \epsilon_1)e^{-k(z+d+z')} + (\epsilon_1 + \epsilon_2)e^{-k(z'-z)}\right], \quad -\frac{d}{2} \leq z < \frac{d}{2}$$
$$g_{III}(z,z',k) = \frac{2\epsilon_2}{k\Delta}e^{-k(z'-z)}, \quad z < -\frac{d}{2}$$
$$\Delta = (\epsilon_1 + \epsilon_2)^2 - (\epsilon_1 - \epsilon_2)^2 e^{-2kd} \tag{22}$$

4.3. GREEN'S FUNCTIONS

The final expressions for the Green's functions may be obtained by inserting the reduced Green's functions of Eqs. (19) and (22) into Eq. (7) or (8). We note that by expanding the denominators (e.g., Δ) in power series we may easily obtain exact expressions for the three dimensional Green's function in the form of infinite image contributions [6]. For instance, the interaction of the two charges in the interior of the protein may be evaluated through the expression:

$$G(\rho,z,z') = \frac{1}{4\pi\epsilon_2}\sum_{n=0}^{\infty}\left(\frac{\epsilon_1 - \epsilon_2}{\epsilon_1 + \epsilon_2}\right)^{2n}\left[\frac{1}{\sqrt{\rho^2 + [2dn + |z - z'|]^2}} + \left(\frac{\epsilon_1 - \epsilon_2}{\epsilon_1 + \epsilon_2}\right)^2\frac{1}{\sqrt{\rho^2 + [2d(n+1) - |z - z'|]^2}}\right.$$
$$\left. - \left(\frac{\epsilon_1 - \epsilon_2}{\epsilon_1 + \epsilon_2}\right)\left\{\frac{1}{\sqrt{\rho^2 + [2d(n+1/2) - (z+z')]^2}} + \frac{1}{\sqrt{\rho^2 + [2d(n+1/2) + (z+z')]^2}}\right\}\right] \tag{23}$$

Instead of writing explicitly these long expressions, we to integrate numerically Eq. (7) for the reduced Green's functions; the latter numerical approach is generalizable to more complex geometries as well.

In Figure 4 we compare the electrostatic interaction energy between two unit charges located in the interior of the protein slab with that when the charges are embedded in an infinite medium with the same dielectric constant as the protein. We observe that the introduction of the two interfaces reduces dramatically the electrostatic interaction between the charges. We note in the calculations we did not include the self-interaction terms of the charges with the surfaces since the latter do not affect the direct exchange between the two charges. In the figure we consider a kinesin slab of length 5 nm and place the charge in the interior an close to the surface at distances 1 Å (dot-dashed line) and 5 Å (dotted line) respectively. We note that close to the other surface of the protein located at $z = -2.5$ nm the electrostatic energy is in the thermal noise level. Specifically we see that the electrostatic interaction becomes of order

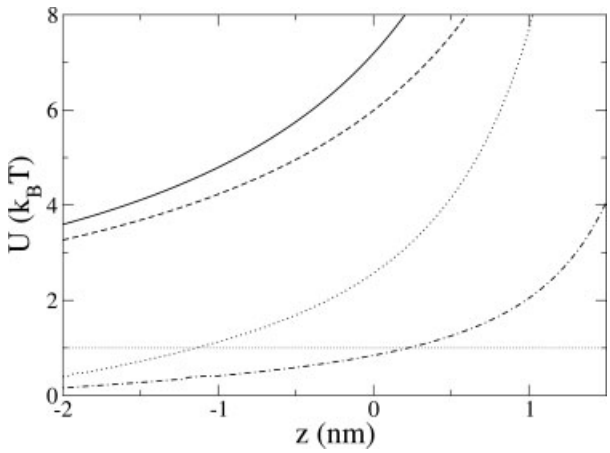

FIGURE 4. Electrostatic interaction energy U (in k_BT at room temperature) as a function of the charge distance z (in nm) for a protein slab with length 5 nm, located in the range $[-2.5, 2.5]$ nm and comparison with corresponding energies for the infinite medium with permittivity ϵ_2. For a unit charge located at $z_1' = 2.4$ nm, i.e., at a distance 1 Å in the interior of the protein (dot-dashed line); infinite medium energy (dashed line). For a unit charge located at $z_2' = 2$ nm, i.e., at 5 Å from the interface (dotted line); infinite medium energy (solid line). The dotted line parallel to the z-axis marks the thermal energy k_BT at room temperature.

k_BT at the length scale $l \simeq 3$ nm and decays beyond this value at larger distances. In the more relevant case of a protein slab with $d = 8$ nm we see from Figure 5 a similar behavior but with a scale of the order $l \sim 4$ nm for dropping the energy at the k_BT level.

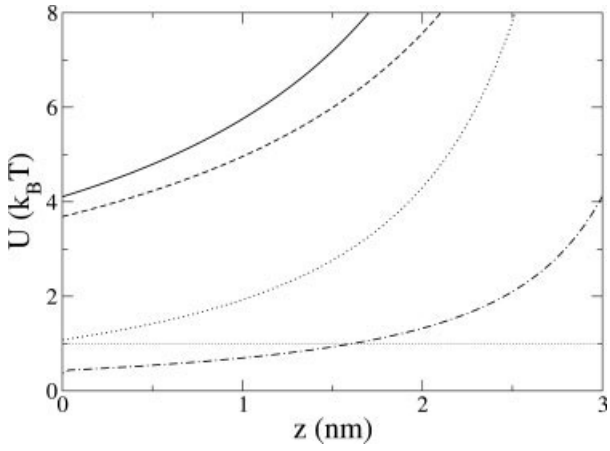

FIGURE 5. Same as in Figure 3 for a protein slab with $d = 8$. For a unit charge is located at $z_1' = 3.9$ nm (dot-dashed line); infinite medium energy (dashed line). For a unit charge located at $z_2' = 3.5$ nm (dotted curve); infinite medium energy (solid line).

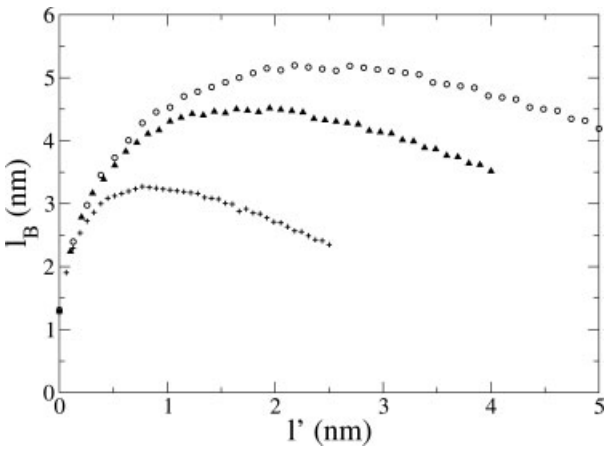

FIGURE 6. Bjerrum length l_B in the interior of the kinesin protein model ($\epsilon = 4$) as a function of the distance l' of the source charge from the medium-protein interface located at $z = d/2$ ($l' = d/2 - z'$). The second (test) charge is placed at distance l_B from the source charge. Dielectric self-energies are not included, only the direct charge–charge Coulomb energy. Three protein slab lengths are considered, $d = 10$ nm (upper curve-circles), $d = 8$ nm (middle curve-triangles) and $d = 5$ nm (lower curve-crosses).

It is useful to analyze in more detail the dependence of the protein Bjerrum length on the distance of the unit charge from the interface. We recall that when two unit charges are placed at a distance l_B equal to the Bjerrum length in dielectric medium then their electrostatic energy is equal to k_BT at room temperature. For water, we have $l_B \simeq 0.7$ nm while if the protein medium ($\epsilon \simeq 4$) were infinite we would have $l_B \simeq 14$ nm; the presence of the interfaces changed drastically this last figure. In Figure 6, we plot the true Bjerrum length in the slab protein model as a function of distance of the source charge from one of the surfaces and in the interior of the protein. We note that when the charge is within an Angstrom from the surface the image charges are very strong and the Bjerrum length very small. This feature changes rapidly within few Angstroms and indeed we see that at a distance 0.5 nm form the dielectric surface the Bjerrum length increases to $l_B \approx 3$ nm (for $d = 5$ nm). The nonmonotonicity of the Bjerrum curve is noteworthy as well as the fact that it reaches a maximum well before the middle of the protein. These features clearly depend on the competition between the screening scale and the actual size of the protein. For a slab size closer to the kinesin dimer, i.e., for $d = 8$ nm we observe that the Bjerrum length is substantially larger compare to the $d = 5$ nm case

reaching a maximum of approximately $l_B \simeq 4.5$ nm. The Bjerrum length thus depends strongly not only on the distance of the source charge from the surface but also on the actual size of the protein because the latter determines the effect of the second interface whose presence increases screening. As the size of the protein increases the effect of the second interface diminishes and the Bjerrum length increases, as expected.

5. Conclusion

From the analysis of the simple one interface model we found that the energy of a charge near the surface but in the interior of the protein is substantially different compared with the case when it is just in the exterior. In either case, we saw the energies involved are close to the thermal energy. Subsequently we analyzed a model that contains two interfaces that is closer to the protein features. We found that the energies in the interior are substantially smaller compared with those if the medium were infinite; i.e., the presence of the interfaces reduces the electrostatic interaction [5]. To quantify these features, we calculated the effective Bjerrum length l_B in the interior of the protein for three model protein sizes, viz. $d = 5$ nm, $d = 8$ nm (corresponding approximately to the kinesin dimer size), and $d = 10$ nm. We found that l_B is quite small within few Angstroms from the interface, yet, increases rapidly reaching a value larger than 4 nm (for $d = 8$ nm) as the charge is moved slightly in the interior. The Bjerrum length depends strongly not only on the distance from the surface but also the actual size of the protein because this determines the effect of the second interface whose effect is to increase screening. As the size of the protein increases the effect of the second interface diminishes and the Bjerrum length increases, as expected. This dependence of the Bjerrum length on distance plays an important role in the energetics of the kinesin walk that will be discussed later.

Dimeric kinesin is a motor protein that hydrolyzes ATP and moves along protofilaments of microtubules with speeds reaching 500 nm/s. Intense experimental work over the last 10 years has shed light in many aspects of the kinesin walk including specific features of motion and its dependence on ATP. Nonetheless, the physics of the energy pathway that starts with the ATP hydrolysis circle and ends with a kinesin translational step is not known. Most available kinesin theoretical models are based either on simple mechanical schemes or deal directly with the various reaction rates entering in the kinesin walk.

Recently, we introduced an electrostatic model for kinesin that goes beyond the simple phenomenological models [2]. In this model, the kinesin motion results from the changes of charges in the ATP and ADP binding sites as well as the overall electric charge distribution of the microtubule. More specifically, it was shown that the kinesin dimer is bound to the negatively charged microtubule due to positive excess charge in one kinesin head whereas the tethered head has an axes of negative charge due to presence of ADP. On ATP capture and hydrolysis, the local charge in the bound head changes to negative and thus the head is repelled from the microtubule. At the same time, experiments show that ADP is expelled from the tethered head and, as a result, the remaining local positive charge makes the head fall toward the microtubule due to the generated attraction. The motion thus of kinesin is seen as the coordinated rotational and translation of a fluctuating electrical dipole. Special role in this process plays the charge distribution of the neck region that is positive in the case of kinesin and thus assists in the stability of the walk. Finally, the microtubule dipole moment plays fundamental role in the directionality of the motion.

Although the electrostatic model is qualitatively compatible with all known features of the kinesin walk, one needs to address several specific issues it raises before a complete physical picture of the walk emerges. One such issue is related to the mechanism of ADP expulsion after the ATP capture. Although one may assume that in some fashion part of the ATP hydrolysis energy is used for this process, the precise way this occurs cannot be addressed easily. One may, for instance, invoke coherent vibrational energy transfer mechanisms, such as the ones studied by Davydov and Scott, or direct charge transfer, as seems to occur in other macromolecule [9, 10]. An alternative process, which might be to some extent responsible for the ATP expulsion from the tethered kinesin head, is the direct electrostatic repulsion from the ATP molecule that enters and gets hydrolyzed at the binding site.

The kinesin walk depends at least in part on electrostatic interactions [2]; this is hardly a surprise since microtubules, on which the walk takes place, are highly charged and polarized and kinesin itself has inhomogeneous surface charge distributions. As the fluctuating charge model is shown to be compatible with numerous experimental data it is necessary

to begin a quantitative search that will lead to precise knowledge of the factors involved in the walk. This is of course a difficult feat because it depends on detailed microscopic kinesin information as well as specific experiments addressing electrical features of the molecule. One feature of the fluctuating charge model is related to the possible connection of the ATP entry to the kinesin binding pocket with the ADP expulsion. Although this correlated event may depend on a variety of factors such as conformational changes, vibrational and/or electron transfer it might has also an electric component stemming from the direct electrostatic APT–ADP interaction. In the present short note we explored the electrostatic aspect of this interaction. Specifically we calculated the exact Green's functions for few simple configurations modeling kinesin focusing particularly on the role of the protein-water interfaces.

To apply the present results to kinesin we may take into account that after hydrolysis the ATP molecule carries approximately three electronic charges while ADP two. As a result, if the two molecules are assumed to be at a distance or order $l \simeq 5$ nm from each other, then the effective interaction between them is of the order of $2-5\,k_BT$, depending on their proximity to the dielectric interfaces. This energy should be compared with the ATP hydrolysis energy that is of the order of $12\,k_BT$, although, a part of this energy is consumed entropically [11]. The rest induces in part local conformational changes leading to the ATP capture as well as other, more extreme, possibilities such as vibrational selftrapping [10] or even polaronic charge transfer [12]. We thus find that although the ATP–ADP electrostatic interaction does not appear sufficient for the ADP expulsion, it seems that it does participate in the process.

Although the analytical expressions and estimates obtained are useful they should be further substantiated through more precise microscopic modeling that also involve screening effects [13] to obtain a clearer quantitative physical picture of the mechanisms involved. Specifically for kinesin the head–head electrostatic interaction is not only due to the mutual repulsion of the nucleotides but also due to the presence of the highly charged tubulin. In Ref. 2 the vertical parked state of kinesin is found to be a consequence of the tubulin-ADP repulsion. As a result, the ADP release rate may be enhanced by the presence of an ATP in the attached head, which is already repelled by the -27 electronic charges localized along the C-terminus of the filament dimer [14]. In the present model, we only address the interaction between two charged nucleotides in two distant locations of the protein; however, the interaction with the charged microtuble surface should also be included. Finally, the presence of salt ions in the surrounding medium are responsible for Debye screening. Although in this work we have focused purely on electrostatic effects due to dielectric discontinuities a complete analysis will have to include ionic effects and screening as well as the role of thermal fluctuations.

References

1. Carter, N. J.; Cross, R. A. Nature 2003, 435, 19.
2. Ciudad, A.; Sancho, J. M.; Tsironis, G. P. J Biol Phys 2006, 32, 455.
3. McLaughlin, S.; Aderem, A. Trends Biochem Sci 1995, 20, 272.
4. Serber, Z.; Ferrell, J. E. Cell 2007, 128, 441.
5. Kirkwood, J. G. J Chem Phys 1934, 2, 351.
6. Iversen, G.; Kharkats, Y. I.; Ulstrup, J. Mol Phys 1998, 94, 297.
7. Schiwinger, J.; DeRaad, L. L.; Milton, K. A. Jr.; Wu-yang Tsai, Classical Electrodynamics; Perseus Books: Reading, 1998.
8. Jackson, J. D. Classical Electromagnetics; Wiley: Ney York, 1962.
9. Davydov, A. S. J Theor Biol 1977, 66, 379.
10. Scott, A. C. Phys Rep 1992, 217, 1.
11. Ciudad, A.; Sancho, J. M. Biochem J 2005, 390 345.
12. Hevré, G.; Aubry, S. Phys D 2006, 216, 235.
13. Winkler, R. G.; Cherstvy, A. G. Phys Rev Lett 2006, 96, 066103.
14. Tuszynski, J. A.; Luchko, T.; Carpenter, E. J.; Crawford, E. J Comput Theor Nanosci 2005, 1, 392.